ELSEVIER

Journal of Nuclear Materials 266–269 (1999) 91–98

journal of nuclear materials

SOL width scaling from consideration of edge transport in tokamaks

G.F. Counsell [a,*], J.W. Connor [a], S.K. Erents [a], A.R. Field [a], S.J. Fielding [a], B. La Bombard [b], K.M. Morel [c]

[a] *UKAEA/EURATOM Fusion Association, Culham Science Centre, Abingdon, Oxfordshire OX14 3DB, UK*
[b] *Plasma Fusion Center, MIT, Cambridge, MA 02139, USA*
[c] *Imperial College of Science, Technology and Medicine, London SW7 2BZ, UK*

Abstract

A simple two-point representation of the tokamak scrape-off layer (SOL), based on the parallel and perpendicular energy balance equations, has been used to develop heat flux width scalings for a wide variety of $\chi_\perp$ models in terms of B_ϕ, n_{sep}, q_{95}, P_{SOL}, R and a. These scalings have been tested against databases of SOL parameters established on COMPASS-D (which exhibits a collisionless SOL), JET Mk IIa divertor and Alcator C-MOD (both of which exhibit strongly collisional SOLs). The better fit scalings to the collisionless dataset all show a positive dependence of SOL width on q_{95} and an inverse dependence on n_{sep}. Four of the better fit scalings also show a positive dependence on P_{SOL} and a strong inverse dependance on B_ϕ. In the collisional case a group of 5 models, each with a $\chi_\perp \propto T^{1/2}/n$ dependence, provide the better fit scalings to *both* collisional datasets. The derived scalings exhibit a strong inverse dependence on P_{SOL} but are independent of B_ϕ, unlike scalings derived from the commonly used Bohm diffusion model, and four of the five are also independent of n_{sep}.

Keywords: SOL modeling; SOL thickness; Transport coefficients

1. Introduction

In attached divertor scenarios, the width (Δ) of the scrape-off layer (SOL) characterises the impacted target area and hence power loadings onto material surfaces. It also plays a role in determining access to the conditions necessary for advanced divertor concepts, such as radiating and detached divertors.

Profiles of density and temperature in the mid-plane SOL, and hence Δ, are determined by a competition between transport processes perpendicular and parallel to the magnetic field. Parallel transport is assumed to be classical and results from either parallel streaming in the collisionless case ($\nu^* <\sim 1$, where $\nu^* = L_\parallel/\lambda_{mfp}$, λ_{mfp} = collisional mean free path and $L_\parallel$ = parallel connection length) or parallel diffusion in the collisional case ($\nu^* \gg 1$). Perpendicular transport, which may be anomalous, can be characterised by a cross-field thermal diffusivity $\chi_\perp$.

In general, the tokamak SOL is fully three-dimensional and involves a plethora of physical processes. Sophisticated codes such as B2-EIRENE are needed to make predictions for the ITER SOL but are hampered by the lack of a physical basis for $\chi_\perp$ and its scaling with plasma parameters.

Several models for $\chi_\perp$, including Bohm and Gyro–Bohm diffusion, were integrated into a simple representation of the SOL [1] to develop scalings for Δ in terms of the key plasma operating parameters. In this paper, the work is extended to investigate a much broader range of models for $\chi_\perp$, requiring a greater variety of parameters in the scalings. The scalings, and hence the applicability of the various $\chi_\perp$ models, are tested against experimental databases of SOL parameters established on COMPASS-D, JET and Alcator C-MOD.

* Corresponding author. Tel.: +44-1 235 463602; Fax: +44-1 235 463770; e-mail: glenn.counsell.cc@ukaea.org.uk

0022-3115/99/$ – see front matter
PII: S0022-3115(98)00880-0

2. Theory

2.1. Simple SOL model

Power into the SOL $P_{\rm SOL} = q_{\|}A_{\|} = q_{\perp}A_{\perp}$, where $q_{\|,\perp}$ are the parallel and perpendicular power densities, $A_{\|}$ is the projection perpendicular to the field line of an annulus width $\Delta_{\rm h}$ at the outboard mid-plane and $A_{\perp}$ is the surface area of the plasma boundary. $\Delta_{\rm h}$ is the SOL heat flux width.

$A_{\|} = 2\pi(R+a)\Delta_{\rm h}\sin(\alpha)$, where α is the field line angle, R and a are the major and minor radii respectively. In the large aspect ratio (LAR) circular approximation, $a \ll R$ and, $\sin(\alpha) = B_{\rm p}/B$, where $B_{\rm p}$ and B are the poloidal and total fields respectively. Thus $A_{\|} = 2\pi R\Delta_{\rm h}B_{\rm p}/B$. Also, in the LAR circular approximation $A_{\perp} = 2\pi R \cdot 2\pi a = 4\pi^2 Ra$.

Now $q_{\perp} = -n\chi_{\perp}\nabla_{\perp}T$. The perpendicular temperature gradient $\nabla_{\perp}T \sim -T_b/\Delta_T$, where T_b is the mid-plane separatrix temperature and Δ_T is the average temperature gradient length (assumed $\propto \Delta_{\rm h}$). Thus,

$$n\chi_{\perp}\frac{T_b}{\Delta_T} = \frac{P_{\rm SOL}}{4\pi^2 Ra}. \tag{1}$$

Similarly $q_{\|} = -k_{\|}\nabla_{\|}T$, where $k_{\|}$ is the parallel heat conductivity and is expressed as $n\chi_{\|}$ to be consistent with the perpendicular case. Thus,

$$-n\chi_{\|}\nabla_{\|}T = \frac{B}{B_{\rm p}}\frac{P_{\rm SOL}}{2\pi R\Delta_{\rm h}}. \tag{2}$$

For classical parallel transport and in the case of a collisionless SOL, parallel streaming gives $\chi_{\|} \propto L_{\|}v_{\rm th} \propto L_{\|}T^{1/2}$, where $L_{\|}$ is the parallel connection length (which is assumed $\propto Rq_{95}$, a LAR approximation). In the collisional case, parallel diffusion gives $\chi_{\|} \propto \lambda_{\rm ee}v_{\rm th} \propto T^{5/2}/n$.

From micro-turbulence arguments the cross-field diffusion coefficient is conveniently modelled as

$$\chi_{\perp} = \chi_{\perp_0}T^{\alpha}/L_{p,T,n}^{\gamma}, \tag{3}$$

where $\chi_{\perp_0} \propto n^{\delta}q^{\mu}R^{\nu}a^{\sigma}B^{\rho}$ and L_p, L_T and L_n are the various perpendicular gradient lengths contained in some of the theoretical expressions for $\chi_{\perp}$.

Making the LAR assumption $B_{\rm p} \sim aB/Rq$ and the simplifying assumption $\nabla_{\|}T \sim T/L_{\|}$ with Eq. (1) and Eq. (2) yields the simple relation $\Delta_{\rm h}^2 \propto L_{\|}^2\chi_{\perp}/\chi_{\|}$. This becomes

$$\Delta_{\rm h} \propto \sqrt{\chi_{\perp}L_{\|}/T^{1/2}} \tag{4}$$

for a collisionless SOL and

$$\Delta_{\rm h} \propto L_{\|}\sqrt{\chi_{\perp}n/T^{5/2}} \tag{5}$$

in the collisional case.

Eqs. (4) and (5) are used to determine $L_{p,T,n}(\sim \Delta_{p,T,n} \propto \Delta_{\rm h})$ in a self-consistent fashion. Although parallel particle transport takes place at the sound speed, L_n is assumed to be governed by Eq. (4) only for a collisionless SOL, in which L_T and L_p are governed by the same equation. In the collisional case strong recycling at the divertor is assumed to result in comparable L_n, L_T and L_p, governed by Eq. (5).

2.2. SOL width scalings

Twenty-one models for $\chi_{\perp}$ have been considered [2], including those based on the effects of resistivity on ballooning and interchange modes, drift turbulence, temperature gradient instabilities and so on. The procedures detailed above were used to obtain scalings for $\Delta_{\rm h}$ in terms of $B(B_{\phi})$, $q(q_{95})$, R, a, $P(P_{\rm SOL})$ and $n(n_{\rm sep}$, the upstream separatrix density) for each $\chi_{\perp}$ model (in the collisional SOL case, five of the $\chi_{\perp}$ models gave rise to two separate scalings as a result of two possible choices for the associated perpendicular gradient length). In addition, and for completeness, three SOL models which estimate the width directly were also considered [2]. Thus twenty-four collisionless and twenty-nine collisional scalings were derived.

3. Experiment

3.1. SOL width databases

3.1.1. COMPASS-D

A detailed study of the variation of SOL heat flux width, $\Delta_{\rm h}$, with plasma parameters has been made in single-null divertor plasmas on the COMPASS-D tokamak. A database has been established of $\Delta_{\rm h}$ against axial toroidal field B_{ϕ}, q_{95}, R, minor radius a, power flowing into the SOL $P_{\rm SOL}$ and electron density at the separatrix $n_{\rm sep}$. $\Delta_{\rm h}$ values were evaluated using measurements from three diagnostics: an array of domed Langmuir probes across the strike point region in one of the divertor tiles, a fast reciprocating triple probe at the top of the vessel and HELIOS [3], a newly installed diagnostic which gives local n_e and T_e values at the mid-plane from helium line ratios (Fig. 1). Data from the probe systems were mapped to the mid-plane assuming pressure balance along flux tubes, a reasonable assumption since collisionality in the COMPASS-D SOL ranges from $0.2 < \nu^* < 3$ (i.e. broadly collisionless) and the SOL does not exhibit detachment from the strike-points.

In order to provide extensive testing of the SOL width scalings, the widest possible range of parameters was explored. Eighty four measurements are so far included with $1.6\times10^{18}\ {\rm m}^{-3} < n_{\rm sep} < 1.6\times10^{19}\ {\rm m}^{-3}$, $0.08\ {\rm MW} < P_{\rm SOL} < 0.7\ {\rm MW}$, $0.8\ {\rm T} < B_{\phi} < 2.1\ {\rm T}$ and $3 < q_{95} < 14$. R and a are essentially fixed at ~ 0.57 m and ~ 0.17 m, respectively, by the geometry of the

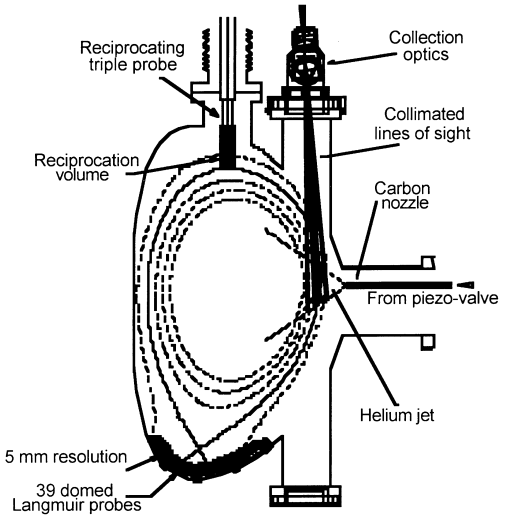

Fig. 1. Schematic showing SOL diagnostics available on the COMPASS-D tokamak. These include an array of target probes, a reciprocating probe at the top of the vessel and the newly installed HELIOS He line ratio diagnostic at the mid-plane.

COMPASS-D vessel. Both Ohmic and ECRH heated plasmas were investigated but no H-mode data are currently included in the database.

3.1.2. JET

A database of upstream values for Δ_h has been formed for JET operation with the Mk IIa divertor configuration [4]. Upstream values are obtained by mapping from measurements made at the divertor target using an array of Langmuir probes across the strike point region. Since JET exhibits a collisional SOL ($20 < v^* < 180$), the mapping is non-trivial and uses the DIVIMP/NIMBUS onion-skin model with benchmarking under suitable conditions against the reciprocating probe.

The JET database currently includes twenty four Ohmic, L-mode (NBI heated) and H-mode shots spanning 3.5×10^{18} m^{-3} $< n_{sep} < 3.9 \times 10^{19}$ m^{-3}, 0.4 MW $< P_{SOL} < 15.8$ MW, 1 T $< B_\phi < 3.5$ T, $2.4 < q_{95} < 4.3$ and with R and $a \sim 3$ m and ~ 1 m respectively.

3.1.3. Alcator C-MOD

The extreme nature of the Alcator C-MOD SOL, at twice the toroidal field of most other machines and with up to an order of magnitude higher separatrix densities, makes it invaluable for extending the testing of Δ_h scalings. For a small machine, the SOL is highly collisional ($22 < v^* < 370$), which allows for scalings with R and a to be tested by comparison with larger, collisional SOL devices such as JET.

A database of edge parameters on Alcator C-MOD has been formed which currently includes 76 Ohmic shots [5,6]. Upstream densities and temperatures across the SOL were obtained with high spatial resolution using a fast reciprocating in an upstream location. The database provides eight measurements of SOL parameters (including local values for the connection length) across a 10 mm radial section of the SOL.

There is a substantial radial variation of the calculated scale-lengths in the Alcator C-MOD database. Although a radial variation in Δ_h is often seen in other tokamak SOLs, it usually only occurs far out into the SOL and is sometimes identified with a change in the dominant heat transfer mechanism from conduction to convection. In Alcator C-MOD, the radial variation is continuous throughout the SOL. Close to the separatrix the values of Δ_h (that is, the local $1/e$ width) are typically 1–2 mm, very much narrower than in, for instance, JET or COMPASS-D. However, the local scale-length gradually increases and, within only 5–10 mm, the local value of Δ_h typically rises to 1 cm.

The separatrix values, which are most often quoted [5,6], do not alone provide a particularly good dataset for testing the SOL width scalings as the key parameters span a relatively narrow range (5.7×10^{19} m^{-3} $< n_{sep} < 1.8 \times 10^{20}$ m^{-3}, 0.4 MW $< P_{SOL} < 1.2$ MW, 2.8 T $< B_\phi < 7.9$ T and $3.3\ q_{95} < 5.1$). However, the high radial resolution of parameters provided in the dataset allows, with some assumptions, each of the eight local measurements for each entry to be used.

In practice, we treat the flux tube at each of the radial measurements as an individual SOL. The local density and heat flux scale-length are used in place of n_{sep} and Δ_h. The local connection length divided by $2\pi R$ is used to calculate a local q_{local}, in place of q_{95}. Lastly, the power flow into the flux tube is estimated by a simplified onion skin model ($P_{n+1} = P_n - \int_{r_n}^{r_{n-1}} P_n e^{-r/\lambda_{P_n}} dr$, where P_n is the power flow into the nth flux tube and is equal to P_{SOL} at the separatrix. λ_{P_n} is the local heat flux scale-length in the nth flux tube). With these assumptions the parameter range is greatly enhanced to 1.3×10^{19} m^{-3} $< n < 1.8 \times 10^{20}$ m^{-3}, 0.01 MW $< P < 1.2$ MW, 2.8 T $< B_\phi < 7.9$ T and $3.3 < q_{local} < 19.5$, with R and $a \sim 0.67$ m and ~ 0.21 m respectively. Forty-nine of the Alcator C-MOD database entries are suitable for this analysis, yielding 392 values.

The range of parameters accessed by the COMPASS-D, JET Mk IIa divertor and Alcator C-MOD SOL databases is summarised in Table 1.

4. Scaling tests

Many attempts have been made in the past to extract trends and relationships from SOL databases. These analyses are usually performed using multivariate fitting algorithms between two or more SOL parameters. Although they can provide helpful information, and may

Table 1
Summary of parameters encountered in the COMPASS-D, JET and Alcator C-MOD (separatrix only and across the SOL values) databases

	COMPASS-D	JET Mk II	Alcator C-MOD	
			Sep. Only	All SOL
ν^*	0.2–3	20–180	22–370	22–370
n_{sep} (10^{18} m^{-3})	1.6–16	3.5–39	57–180	13–180
P_{SOL} (MW)	0.09–0.7	0.4–15.8	0.4–1.2	0.01–1.2
q_{95}	3–14	2.4–4.3	3.3–5.1	3.3–19.5
B_ϕ (T)	0.8–2.1	1–3.5	2.8–7.9	2.8–7.9
R (m)	0.57	3	0.67	0.67
a (m)	0.17	1	0.21	0.21

be useful for extrapolation, they suffer from the fundamental problem of collinearity between parameters. For instance, local densities, temperatures and heat fluxes may be inextricably linked (on JET, the upstream values of density and temperature are, in fact, found to be linearly related [7]) as are, of course, parameters such as B_ϕ, q_{95} and I_P. These, and many other collinearities, mean that any scalings detected by multivariate fits to data are likely to contain parameter indices which are not directly related to the underlying physics.

The scaling tests performed here are a fundamentally different approach. In this work, the physics has been used a priori to derive the scalings, which thus implicitly and correctly include the effect of collinearities. The scalings can then be compared for their ability to fit the data in order to investigate possible underlying physical processes.

4.1. Method of evaluation

A simple quality of fit parameter, such as the Pearson R^2 value, is inappropriate to rank the scalings for several reasons. Firstly, there is no provision for an offset in the scalings, $\Delta_h \propto f(B_\phi, R, a, P_{SOL}, n_{sep})$. The fit must therefore be constrained to pass through the origin. Secondly, any ranking must account for experimental errors, not only in the measured SOL width but also in the measurement of plasma parameters used in the scalings. Thirdly, some account must be made for grouping of the data in parameter space. That is, to account for the fact that much of the experimental data often lies within relatively narrow parameter ranges.

Realistic errors have been assigned to each of the 'independent' variables B_ϕ, q_{95}, R, a, n_{sep} and P_{SOL}, as well as the 'dependent' variable, Δ_h. Fig. 2 shows a plot of measured and scaled Δ_h values for COMPASS-D data with a typical (but poorly fitting) model. Shown on the figure are the error ellipses which represent one standard deviation from each data point (the result of error bars in both the dependent and independent variables), together with a best-fit line to the data.

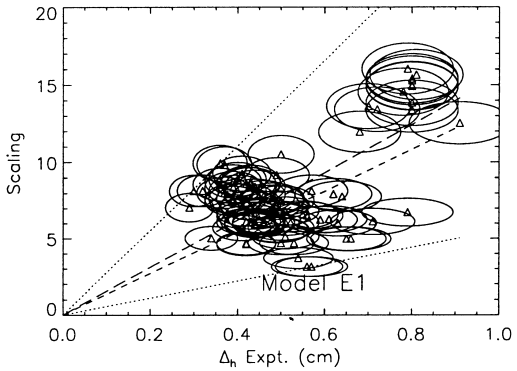

Fig. 2. Plot of typical (but poorly fitting) scaling against measured Δ_h for COMPASS-D data showing error ellipses and the calculated best-fit line (long dash) together with the simple least squares fit line (short dash).

The best-fit line was determined from a minimisation of a quality of fit parameter, ε, which is essentially the sum of the number of standard deviations of each point away from the line (the number of standard deviations until the error ellipse just touches the line). ε is analogous to the usual minimisation parameter for a least squares fit with errors in the dependant variable. In addition, in order to account for grouping of the data in parameter space, each point is weighted by $1/\sqrt{n_{neighbours}}$, where $n_{neighbours}$ is the number of nearest neighbours (those within one standard deviation of the whole data set). The best-fit line cannot be evaluated algebraically and was determined by a binomial search algorithm.

4.2. Collisionless SOL

Twenty-four collisionless scalings for Δ_h were tested against data from the COMPASS-D database.

Fig. 3 shows the value of ε (normalised to 1.0 for the worst model) for the COMPASS-D data for each of the models tested (labelled A–Q). There are two clear groups of models, one with low ε and the other with high ε.

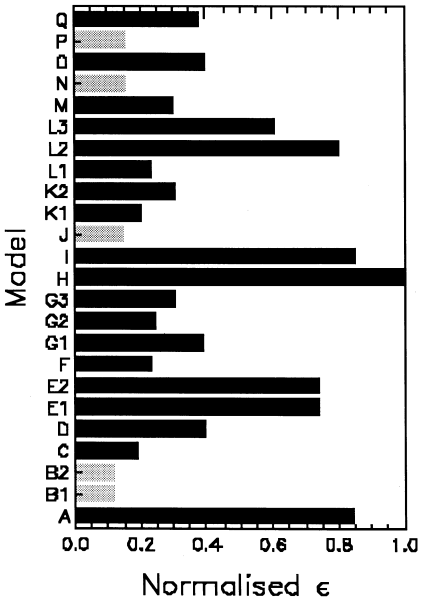

Fig. 3. Ranking of the 24 scalings tested against COMPASS-D (collisionless SOL) data, according to the normalised value of the quality of fit parameter, ε (best model has lowest value of ε).

Models $B1/B2$ (which lead to identical scalings and are thus indistinguishable) stand out, followed by models J, P and N. A similar ranking was provided for an earlier version of the COMPASS-D database [2], in which model J provided the best fit, followed by models D/O (also indistinguishable) and $B1/B2$. However, the earlier database included few points at high values of $q_{95}/n_{\rm sep}$. When this region of parameter space is filled, it is seen that models D/O no longer provide good scalings.

Fig. 4 shows the COMPASS-D data against the scaling for models $B1/B2$. The scaling takes the form $\Delta_{\rm h} \propto B_\phi^{-6/11} q_{95}^{8/11} R^{3/11} a^{-2/11} P_{\rm SOL}^{2/11} n_{\rm sep}^{-2/11}$ and derives from a model for $D_\perp (\sim \chi_\perp)$ based on the effects of sheath resistance on the ideal MHD interchange mode [2] yielding $\chi_\perp \propto qT^{3/2}/B^2 L_p$.

The second best scaling, that for model J, has the simpler form $\Delta_{\rm h} \propto q_{95}^{1/3} R^{1/3} n_{\rm sep}^{-1/3}$ deriving from a model for $D_\perp$ based on the effect of collisionless skin depth on drift wave transport [2] yielding $\chi_\perp \propto T^{1/2}/nL_n$.

All the better fitting scalings, including that for model N (the ubiquitous Bohm transport model, $\chi_\perp \propto T/B$), exhibit a positive dependence on q_{95} and an inverse dependence on $n_{\rm sep}$. Four of these scalings also show a positive dependence on $P_{\rm SOL}$ and a strong inverse dependence on B_ϕ.

4.3. Collisional SOL

Figs. 5 and 6 show the value of ε for JET Mk IIa divertor and Alcator C-MOD SOL data for 29 collisional $\Delta_{\rm h}$ scalings. As in the collisionless case, there are two clear groups of models, one with low ε and the other with high ε. Those developed for models D/O (which lead to identical scalings and are thus indistinguishable), $J3$, M, Q and J provide notably better fits to the Alcator C-MOD data and five of these, models D/O, J, $J3$ and

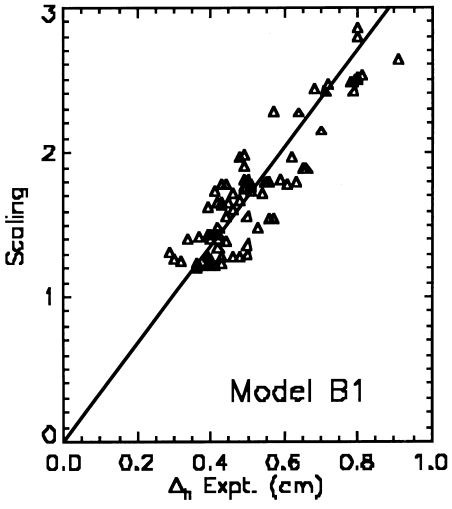

Fig. 4. Plot of COMPASS-D (collisionless SOL) data against the best fit scaling, $\Delta_{\rm h} \propto B_\phi^{-6/11} q_{95}^{8/11} R^{3/11} a^{-2/11} P_{\rm SOL}^{2/11} n_{\rm sep}^{-2/11}$ which derives from a $\chi_\perp$ model based on the effects of sheath resistance on the ideal MHD interchange mode.

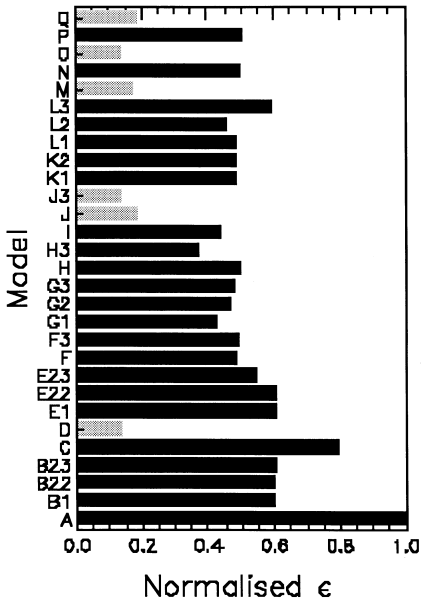

Fig. 5. Ranking of the 29 scalings tested against Alcator C-MOD (collisional SOL) data, according to the normalised value of the quality of fit parameter, ε (best model has lowest value of ε).

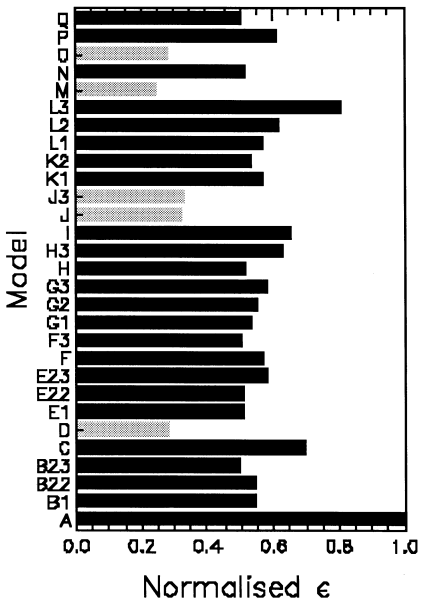

Fig. 6. Ranking of the 29 scalings tested against JET (collisional SOL) data, according to the normalised value of the quality of fit parameter, ε (best model has lowest value of ε).

M, also provide (albeit in a different ordering) the better fits to the JET data.

Fig. 7 shows the Alcator C-MOD data against the scaling for models D/O whilst Fig. 8 shows the JET data for model M, respectively the best-fit models for each

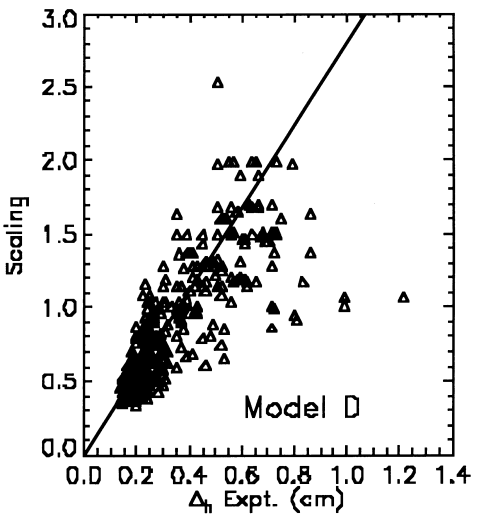

Fig. 7. Plot of Alcator C-MOD (collisional SOL) data against the best fit scaling, $\Delta_h \propto q_{95}^{-1/10} R^{3/10} a^{2/5} P_{SOL}^{-2/5}$ which derives from a $\chi_\perp$ model based on the effects of sheath resistance on interchange modes near a critical value of β.

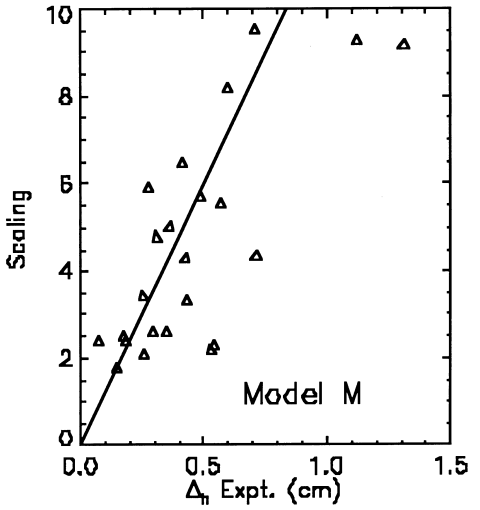

Fig. 8. Plot of JET (collisional SOL) data against the best fit scaling, $\Delta_h \propto q_{95}^{3/5} R a^{2/5} P_{SOL}^{-2/5}$ which derives from a $\chi_\perp$ model which assumes that perpendicular transport arises from charge exchange collisions.

device. The collisional scalings for models D/O take the form $\Delta_h \propto q_{95}^{-1/10} R^{3/10} a^{2/5} P_{SOL}^{-2/5}$. Model D is based on the effects of sheath resistance on interchange modes near a critical value of β, whilst model O uses the collisionless skin-depth as the step-length in a random walk argument [2]. Both yield a perpendicular diffusion coefficient of the form $\chi_\perp \propto T^{1/2}/nRq$.

The collisional scaling for model M, which assumes that perpendicular transport arises from charge exchange collisions yielding $\chi_\perp \propto T^{1/2}/n$, has a similar form $\Delta_h \propto q_{95}^{3/5} R a^{2/5} P_{SOL}^{-2/5}$. Model J relates perpendicular diffusion to the differential motion of the plasma and magnetic surfaces, which becomes significant when the collisional skin depth is comparable to the fluctuation scale length yielding $\chi_\perp \propto T^{1/2}/n$.

All the better fitting collisional scalings exhibit a strong inverse dependence on P_{SOL} but are independent of B_ϕ, unlike scalings derived from the commonly used Bohm diffusion model, and four of the five are also independent of n_{sep}. The associated perpendicular diffusion coefficients all have a $\chi_\perp \propto T^{1/2}/n$ dependence (see Table 3).

Table 2
Extrapolation of simple zero-dimensional model scalings to ITER mid-plane SOL width (values are prone to a large (factor 2) uncertainty)

Database used	D/O (mm)	J (mm)	$J3$ (mm)	M (mm)
Alcator C-MOD	1.5	4.3	3.5	5.1
JET Mk IIa	1.8	3.4	3.6	3.2

Table 3
Better fitting Δ_h scalings for the collisionless and collisional SOL cases, together with the associated $\chi_\perp$ model and a brief description of the physics basis for each of the models

Model	$\chi_\perp$ scaling	Physics basis	Δ_h scaling
Collisionless SOL			
*B*1	$\chi_\perp \propto qT^{3/2}/B^2L_p$	Endplate MHD interchange, $\nabla_\perp \sim L_p$	$\Delta_h \propto B_\phi^{-6/11} q_{95}^{8/11} R^{3/11} a^{-2/11} P_{SOL}^{2/11} n_{sep}^{-2/11}$
*B*2	$\chi_\perp \propto qT^{3/2}/B^2L_n$	Endplate MHD interchange, $\nabla_\perp \sim L_T$	$\Delta_h \propto B_\phi^{-6/11} q_{95}^{8/11} R^{3/11} a^{-2/11} P_{SOL}^{2/11} n_{sep}^{-2/11}$
J	$\chi_\perp \propto T^{1/2}/nL_n$	Drift with collisionless skin depth, $L_n \propto L_T$	$\Delta_h \propto q_{95}^{1/3} R^{1/3} n_{sep}^{-1/3}$
P	–	Simple dimensional estimate	$\Delta_h \propto B_\phi^{-3/7} q_{95}^{4/7} R^{3/7} a^{-1/7} P_{SOL}^{1/7} n_{sep}^{-1/7}$
N	$\chi_\perp \propto T/B$	Bohm	$\Delta_h \propto B_\phi^{-3/7} q_{95}^{4/7} R^{3/7} a^{-1/7} P_{SOL}^{1/7} n_{sep}^{-1/7}$
Collisional SOL			
D	$\chi_\perp \propto T^{1/2}/nqR$	Collisionless MHD interchange near β_{crit}	$\Delta_h \propto q_{95}^{-1/10} R^{3/10} a^{2/5} P_{SOL}^{-2/5}$
O	$\chi_\perp \propto T^{1/2}/nqR$	Collisionless skin depth	$\Delta_h \propto q_{95}^{-1/10} R^{3/10} a^{2/5} P_{SOL}^{-2/5}$
J	$\chi_\perp \propto T^{1/2}/nL_n$	Drift with collisionless skin depth, $L_n \propto L_T$	$\Delta_h \propto q_{95}^{6/17} R^{10/17} a^{4/17} P_{SOL}^{-4/17}$
*J*3	$\chi_\perp \propto qT^{1/2}/nL_n$	Drift with collisionless skin depth, $L_n \neq L_T$	$\Delta_h \propto q_{95}^{11/30} R^{23/30} a^{2/5} P_{SOL}^{-2/5} n_{sep}^{7/30}$
M	$\chi_\perp \propto T^{1/2}/n$	Charge-exchange	$\Delta_h \propto q_{95}^{-3/5} R a^{2/5} P_{SOL}^{-2/5}$

5. Extrapolations to ITER

Great care must be exercised when applying extrapolations from these, or any other, scalings to future devices. A scaling may provide a good fit to data by chance and not because the underlying physics is correct (although this becomes less likely as the range of parameters against which they are tested becomes large enough). Even if the physics *is* correct for the tokamaks against which the scalings are compared, different physics may come into play on other devices. In addition, the measurement of Δ_h is prone to significant experimental error, as is the measurement of several parameters used in the scalings (such as P_{SOL}, which is estimated from the total input power and the radiated power fraction, neither of which is usually known with great accuracy).

With these caveats in mind, estimates for the mid-plane heat flux width on ITER (which will have a collisional SOL) are presented in Table 2 for each of the five better fit collisional scalings and, separately, for each database against which the scalings were tested. The slope of the best-fit line in each case (e.g., that shown on Figs. 7 and 8 etc.) was used to determine the associated coefficient of proportionality. Typical proposed ITER operating values [B_ϕ (5.7 T), n_{sep} (5×10^{19} m^{-3}), q_{95} (3), P_{SOL} (100 MW), R (8 m) and a (3 m)] were then entered in the scalings to derive an estimate for Δ_h.

Since none of the better collisional scalings is dependent on B_ϕ or n_{sep}, the extrapolation is thus dominated by the high value of P_{SOL} in ITER (10 times that on JET and 100 times that on Alcator C-MOD). The estimates are thus likely to be subject to significant errors, perhaps by a factor 2. Nevertheless, this simple zero-dimensional model for Δ_h seems to indicate rather narrow SOL widths of around 5 mm or less at the mid-plane.

6. Conclusions

Table 3 summarises the better fit scalings for the collisionless and collisional SOL cases, together with the associated $\chi_\perp$ model and a brief description of the physics basis for each of the models. A fuller explanation is provided in [2]. The better fit scalings to the collisionless dataset show a positive dependence on q_{95} and an inverse dependence on n_{sep}. Four of these scalings also show a positive dependence on P_{SOL} and a strong inverse dependence on B_ϕ. In the collisional case the better scalings exhibit a strong inverse dependence on P_{SOL} but are independent of B_ϕ, unlike scalings derived from the commonly used Bohm diffusion model, and four of the five are also independent of n_{sep}.

Extrapolations from this simple zero-dimensional model for Δ_h to ITER using the better collisional scalings indicate a narrow (<5 mm) mid-plane SOL heat flux width but may be subject to a large (factor of 2) uncertainty.

Acknowledgements

This work has been jointly funded by Euratom and UK Department of Trade and Industry. JET data was obtained under a task agreement between JET and UKAEA Fusion. One of the authors (B. La Bom.) was supported by US DOE Contract DEA CO2-78 ET5 103 and another (K.M.M.) by UK EPSRC grant 96305109.

References

[1] S.I. Itoh, K. Itoh, Plasma Physics and Controlled Fusion 36 (1994) 1115.
[2] J.W. Connor et al., Comparison of theoretical models for scrape-off layer widths with data from COMPASS-D, JET and Alcator C-MOD, Nucl. Fusion, submitted.
[3] A.R. Field et al., Optimised instrument. for edge T_e and n_e measurements on COMPASS-D tokamak from HeI line intensity ratios, Rev. Sci. Instrum., to be published.
[4] S.K. Erents et al., J. Nucl. Mater. 241–243 (1997) 433.
[5] B. La Bombard et al., J. Nucl. Mater. 241–243 (1997) 149.
[6] B. La Bombard et al., Fusion Energy, vol. 1, IAEA, Vienna, 1996, p. 825.
[7] S.K. Erents, private communication, 1998.